Stabilizer-mediated Synthesis of High Activity PtFe/C Nanocatalysts for Fuel Cell Application

Seung Jun Hwang, Joung Woon Kim, Sung Jong Yoo, Jong Hyun Jang, Eun Ae Cho,
Tae-Hoon Lim, Sung Gyu Pyo,[†] and Soo-Kil Kim[†,*]

Fuel Cell Research Center, Korea Institute of Science and Technology, Seoul 136-791, Korea
*[†]School of Integrative Engineering, Chung-Ang University, Seoul 156-756, Korea. *E-mail: sookilkim@cau.ac.kr*

The sluggishness of the oxygen reduction reaction (ORR) on the Pt surface at the cathode and the accompanying large amounts of Pt necessary to fabricate a single cell have been significant drawbacks in the commercialization of proton exchange membrane fuel cells (PEMFCs). Numerous strategies have been reported for either controlling the electronic structure of the catalyst[1,2] favorable to oxygen reduction or enlarging the surface area of the catalyst[3] by revealing a specific surface crystalline plane,[4] controlling the nanostructure,[5-11] making a transition metal alloy,[12-20] or controlling the particle size and dispersion.[21]

However, in spite of the significant enhancement in the ORR activity, most of the novel nanostructured electrocatalysts can hardly be used in membrane electrode assembly due to difficulties in complex synthesis and in fabricating supported catalysts on carbon. Therefore, Pt-based alloy catalysts on carbon are a promising candidate to replace the pure platinum catalyst in the near future. However, there are barriers to the application such Pt alloy catalysts, such as dissolution of the second metal and the different reducing speed of ions during synthesis due to the different reduction potentials. Studies attempting to overcome the latter problem have focused on adding various types of stabilizer to balance the different reducing speeds.[19,22-27] However, there are numerous candidate transition metals for making Pt-based alloy catalysts including Co, Fe, Ni, and Y. Finding an optimal stabilizer to make these alloys more effectively, i.e., the alloy content, particle size/size distribution, and dispersion on carbon, is a very important prerequisite in the development of an alloy catalyst for PEMFCs. We have recently reported that the PtCo/C alloy catalyst synthesized in the presence of CTAB (hexadecyltrimethylammonium bromide, $C_{19}H_{42}BrN$) as a stabilizer exhibited twice the mass activity toward ORR compared to commercial Pt/C, which is superior to other stabilizer-mediated synthesized PtCo/C catalysts.[20] In this study, as a part of the attempts to find a suitable stabilizer for the synthesis of other Pt-transition metal alloy catalysts, we investigated the use of a series of stabilizers in the synthesis of PtFe/C. We consider that the study results will support the discovery of a universal and effective stabilizer for alloying many transition metals with Pt. Such a stabilizer will support the development of a Pt-

based binary alloy, as well as ternary alloy catalysts with an activity significantly enhanced compared to that of the binary alloy catalyst.[18]

The transmission electron microscopy (TEM) analysis results of the PtFe/C catalysts synthesized with various surfactants are depicted in Figure 1(b) to (d), in comparison with commercial 40% Pt/C catalyst (a). The stabilizers were added to give a content equivalent to 5 times the total molar content of Pt and Fe ions. Since any residual stabilizer on the catalyst surface after synthesis deteriorates the activity of the catalysts by blocking the surface, all PtFe/C catalysts were heat treated to remove the stabilizers from the catalyst surface at either 250 °C (CTAB and TOAB (tetraoctyl-ammonium bromide, $C_{32}H_{68}BrN$)) or 350 °C (OAM, oleyl-amine, $C_{18}H_{37}N$), where these temperatures were predetermined from temperature-programmed reduction. The particle size and size distribution of each catalyst have different aspects. In the case of the commercial Pt/C catalyst (Fig. 1(a)), the Pt nanoparticles of diameter 1 to 5 nm were well
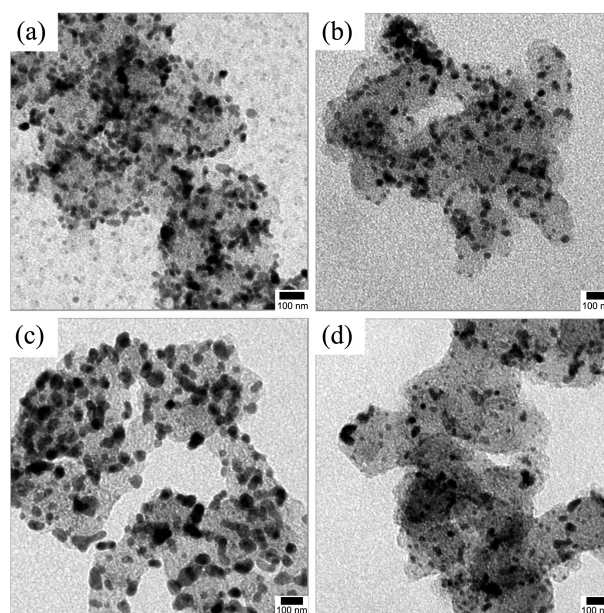

Figure 1. TEM images of commercial Pt/C catalyst (a), and the synthesized PtFe/C catalysts in the presence of OAM (b), CTAB (c), and TOAB (d).

dispersed on carbon supports with sporadic agglomeration. As described above, three different stabilizers were added during the synthesis to co-reduce the Pt^{4+} and Fe^{3+} ions having different reducing potentials. The addition of OAM during the synthesis afforded an alloy composition of $Pt_3Fe_{0.7}$, according to the TEM EDX analysis. As shown in Figure 1(b), the particle sizes were similar to those of the commercial catalyst but the dispersion on the carbon was not homogeneous with many particles being agglomerated. The cationic stabilizer CTAB afforded different particle size and dispersion (Fig. 1(c)). The particle size of PtFe in this case was very uniform in the range of 3 to 5 nm. The average particle size was slightly larger than that of commercial Pt and OAM-mediated PtFe, but the particle dispersion was better than that of OAM-mediated PtFe. The composition of CTAB-mediated particles was $Pt_3Fe_{0.6}$, of which the degree of alloying was slightly lower than in the OAM case. The particle size distribution of TOAB-mediated PtFe/C, shown in Figure 1(d), was from less than 1 nm to 8 nm. Although the degree of alloy was similar to the other cases, i.e., $Pt_3Fe_{0.7}$, the morphology reflected the possibly poor catalytic activity of TOAB-mediated PtFe/C.

The X-ray diffraction (XRD) analysis results of as-synthesized and heat-treated PtFe/C in the presence of various stabilizers are presented in Figure 2. For the as-synthesized PtFe/C catalysts (Fig. 2(a)), the Pt (111) peaks of all samples were shifted to a higher angle by 0.06 to 0.32 degrees compared to that of commercial Pt/C. This was attributed to the lattice contraction of Pt through alloying with the smaller Fe atoms, which reflects the formation of PtFe alloy. The lattice contraction and the consequent stress formation are known to be essential mechanisms for enhancing the ORR
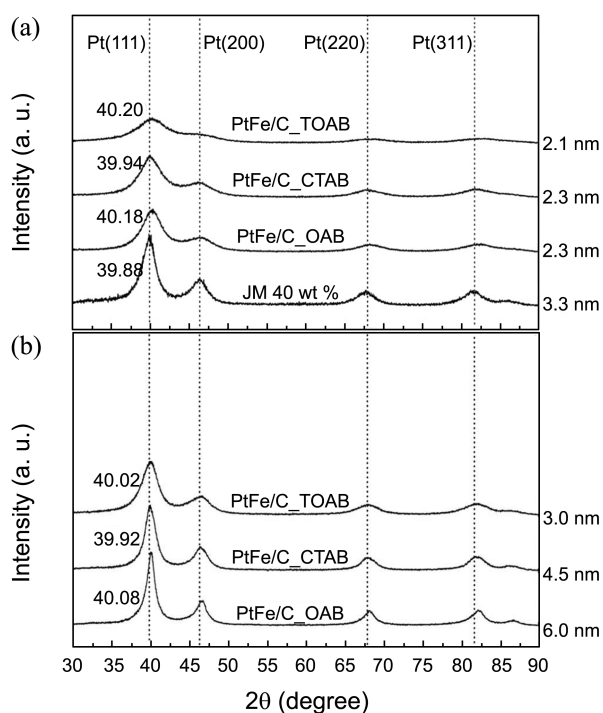
activity of Pt-based catalysts by down-shifting the center of the d-band of Pt and weakening the binding of oxygen-species.[1,12,13] The ORR characteristics of those catalysts will be discussed later. The average particle sizes of the PtFe/C catalysts synthesized in the presence of various stabilizers, as calculated from the full width at half maximum of the Pt (220) peaks, ranged from 2.1 to 2.3 nm without significant variation according to the stabilizer type. These sizes were smaller than that of commercial Pt/C. However, as indicated earlier, the stabilizers used in the alloy synthesis must be removed by heat treatment, which leads to agglomeration of the PtFe nanoparticles. As indicated in Figure 2(b), the particle sizes of heat-treated PtFe/C increased to 3.0 to 6.0 nm. A comparison with Figure 1 reveals a slight discrepancy between the XRD- and TEM-based particle sizes, which was due to the characteristics of the XRD-based calculation in showing the average values of the entire sample. The sporadic agglomeration of PtFe/C-OAM in Figure 1(b) may have caused the large particle size calculated from XRD. Most importantly, however, the heat treatment induced the particle growth without changing the degree of the alloy.

The PtFe/C catalysts synthesized in the presence of various stabilizers were further tested for their ORR activity (Fig. 3). The activity was measured by scanning the potential in the O_2-saturated $HClO_4$ electrolyte. As the potentials were swept in the negative direction, ORR took place at around 0.95 to 1.0 V *vs*. RHE. As the potential was swept further, the curves sequentially passed the kinetic controlled region until 0.9 V, the charge transfer-mass transfer mixed region around 0.8 V and finally the mass transfer-controlled region at the potential negative than 0.8 V. A slight variation in the limiting current densities at mass-transfer controlled region was observed. This is probably due to some experimental factors, for example, non-uniform coating of catalyst inks having different viscosity or dispersion. Though this kind of variation sometimes observed in the literatures,[3,28] it has little effect in the evaluation of

Figure 2. XRD patterns of the synthesized PtFe/C catalysts: (a) as-synthesized and (b) after heat treatment to remove the stabilizers.
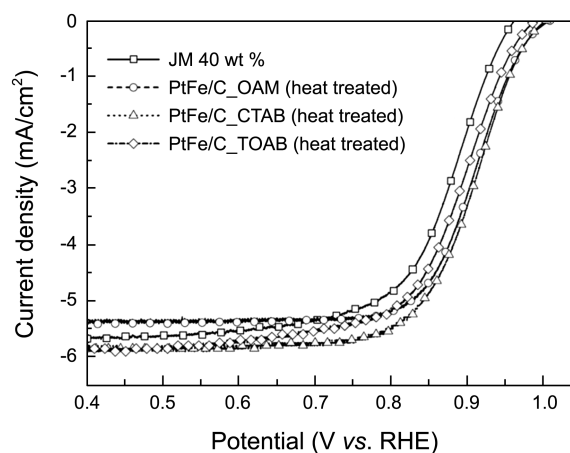

Figure 3. I-V curves for oxygen reduction reaction (ORR) on commercial Pt/C catalyst and three PtFe/C catalysts synthesized using stabilizers. All PtFe/C catalysts were heat treated prior to use. The electrolyte was O_2 saturated 0.1 M $HClO_4$ solution and the working electrode was rotated at 1600 rpm.

Notes

Bull. Korean Chem. Soc. **2012**, Vol. 33, No. 2   701

Table 1. Kinetic current densities at 0.9 V *vs.* RHE and half wave potentials of commercial and synthesized PtFe/C catalysts

Stabilizer	Kinetic current density @ 0.9 V (*vs.* RHE, mA/cm^2)	Half wave potential ($E_{1/2}$, V *vs.* RHE)
no (commercial)	1.99	0.88
OAM	3.15	0.91
CTAB	3.36	0.91
TOAB	2.67	0.89

catalyst activity determined at the kinetic-controlled region.

As indicative of the ORR activity of each catalyst, we measured the kinetic current density at 0.9 V ($i_{k@0.9V}$) and the half-wave potential ($E_{1/2}$) for each catalyst; the results are presented in Table 1. The commercial Pt/C catalyst had $i_{k@0.9V}$ of 1,990 μA/cm^2 and $E_{1/2}$ of 0.88 V. The OAM-mediated PtFe/C catalyst exhibited a 1.6-fold increase in $i_{k@0.9V}$ of 3,147 μA/cm^2 and a slightly increased $E_{1/2}$ of 0.91 V. The increased kinetic current density and half-wave potential revealed the superior ORR activity of the OAM-mediated PtFe/C catalyst, which was mainly attributed to the alloy effects. Similarly, the CTAB-mediated PtFe/C catalyst exhibited the best activity with $i_{k@0.9V}$ of 3,357 μA/cm^2 and $E_{1/2}$ of 0.91 V. Despite the relatively larger particle size of CTAB-mediated PtFe/C compared to OAM-mediated PtFe/C, the better dispersion in combination with the alloy effect may have been responsible for the better activity. However, the kinetic current density and half-wave potential of TOAB-mediated PtFe/C, $i_{k@0.9V}$ of 2,670 μA/cm^2 and $E_{1/2}$ of 0.89 V, were only slightly better than those of the commercial catalyst due to the poor dispersion and agglomeration of the particles, as shown in Figure 1(d). These study results confirmed CTAB as the most suitable stabilizer for the synthesis of PtFe/C electrocatalysts. Nevertheless, the CTAB content should also be considered. Therefore, the effect of CTAB at two different concentrations was investigated. CTAB at 1-fold of the total molar content of Pt and Fe ions (Fig. 4(a)) resulted in a lower degree of alloy (Pt$_3$Fe$_{0.4}$) and a broad particle size distribution. At the larger CTAB concentration of 10-fold (Fig. 4(b)), aggregation occurred possibly due to the hydrophobic interactions between the hydrocarbon chains of the surface-adsorbed CTAB molecules, while no increase in the degree of alloy (Pt$_3$Fe$_{0.6}$) was obtained.
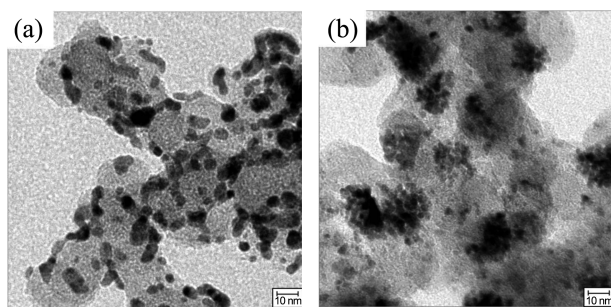
Figure 4. TEM images of the synthesized PtFe/C catalyst with two different CTAB contents: (a) 1- and (b) 10-fold of the total molar content of Pt and Fe ions.

It is difficult to reach a general description about the effects of the stabilizer's molecular structure on the final characteristics of the synthesized PtFe/C with the limited experimental results. It is true that the aspects of stabilizer effect are different according to the target alloy nanoparticles. For example, in the case of PtCo/C in our previous investigation, the ionic state seems to play important roles (that is, CTAB and TOAB-mediated PtCo/C exhibited the better performance than the case of OAM-mediated PtCo/C).[20] However, in the present study while CTAB-mediated PtFe/C exhibited the best activity, which is the same with our previous study, OAM-mediated PtFe/C had the better activity than that of TOAB-mediated one. Since there is no significant difference in the degree of alloy between TOAB and OAM cases, the activity difference between those two cases are mostly due to the particle morphology. Both the hydrophobic interaction from hydrocarbon chain and the electrostatic repulsion from positive charge at nitrogen atom may play the key roles in determining the morphology, of which the details need some more systematic studies.

In summary, we tested three different stabilizers in the synthesis of PtFe/C alloy catalysts for ORR in PEMFC. The synthesized alloy catalysts were analyzed in terms of morphology, crystalline structures, and electrochemical activity. Among the three stabilizers, CTAB was the best for obtaining uniform alloy particle size and excellent dispersion of the particles on the carbon supports. The resulting CTAB-mediated Pt$_3$Fe$_{0.6}$/C catalyst exhibited a 1.7-fold improvement in activity toward ORR compared to that of the commercial Pt/C catalyst.

Experimental Section

10 mL of 0.3 mmol platinum chloride (PtCl$_4$) and 0.1 mmol iron chloride (FeCl$_3$) in anhydrous ethanol were sonicated for 10 min, and then mixed with a previously prepared mixture of 0.97 g Vulcan® XC-72 carbon and 80 ml anhydrous ethanol, followed by another 10 min sonication. Three different stabilizers of OAM (C$_{18}$H$_{37}$N), TOAB (C$_{32}$H$_{68}$BrN), and CTAB (C$_{19}$H$_{42}$BrN) previously dissolved in anhydrous ethanol were added to this mixture to give a content equivalent to 5 times the total molar content of Pt and Fe ions. The precursors were reduced by adding 10-fold amounts of sodium borohydride (NaBH$_4$) as a reducing agent at room temperature under an argon atmosphere. The mixture was aged overnight, filtered, washed with ethanol, and dried for a day at 40 °C in a vacuum oven. The resulting powder was heat treated under an argon-hydrogen mixture atmosphere for 2 h at different temperatures pre-determined from temperature-programmed reduction results.

TEM and XRD analyses were performed to study the morphology, alloy formation, and average size of the synthesized PtFe/C. Electrochemical activity measurement was performed in an oxygen-saturated 0.1 M HClO$_4$ solution using a conventional three-electrode system composed of a saturated calomel electrode, Pt mesh, and a glassy carbon electrode as the reference, counter, and working electrodes.

The working electrode was previously coated with the catalyst ink solution composed of isopropyl alcohol, Nafion® solution (0.1 mL), and the synthesized catalyst powders. The catalyst ink was dried to remove the solvent before use. The glassy carbon electrode was rotated during the experiments at a speed of 1600 rpm and the current was measured while the potential was swept in the range of 0.4 to 1.1 V with respect to reversible hydrogen electrode (RHE).

References

1. Kitchin, J. R.; Nørskov, J. K.; Barteau, M. A.; Chen, J. G. *J. Chem. Phys.* **2004**, *120*, 10240.
2. Ruban, A.; Hammer, B.; Stoltze, P.; Skriver, H. L.; Nørskov, J. K. *J. Mol. Catal. A: Chem*. **1997**, *115*, 421.
3. Lim, B.; Jiang, M.; Camargo, P. H. C.; Cho, E. C.; Tao, J.; Lu, X.; Zhu, Y.; Xia, Y. *Science* **2009**, *324*, 1302.
4. Stamenkovic, V. R.; Fowler, B.; Mun, B. S.; Wang, G.; Ross, P. N.; Lucas, C. A.; Markoviæ, N. M. *Science* **2007**, *315*, 493.
5. Zhai, J.; Huang, M.; Dong, S. *Electroanalysis* **2007**, *19*, 506.
6. Wei, Z. D.; Feng, Y. C.; Li, L.; Liao, M. J.; Fu, Y.; Sun, C. X.; Shao, Z. G.; Shen, P. K. *J. Power Sources* **2008**, *180*, 84.
7. Koh, S.; Strasser, P. *J. Am. Chem. Soc.* **2007**, *129*, 12624.
8. Wang, J. X.; Inada, H.; Wu, L.; Zhu, Y.; Choi, Y.; Liu, P.; Zhou, W.-P.; Adzic, R. R. *J. Am. Chem. Soc.* **2009**, *131*, 17298.
9. Zhang, H.; Yin, Y.; Hu, Y.; Li, C.; Wu, P.; Wei, S.; Cai, C. *J. Phys. Chem. C* **2010**, *114*, 11861.
10. Sarkar, A.; Manthiram, A. *J. Phys. Chem. C* **2010**, *114*, 4725.
11. Chen, Z.; Waje, M.; Li, W.; Yan, Y. *Angew. Chem. Int. Ed.* **2007**, *46*, 4060.
12. Greeley, J.; Stephens, I. E. L.; Bondarenko, A. S.; Johansson, T. P.; Hansen, H. A.; Jaramillo, T. F.; Rossmeisl, J.; Chorkendorff, I.; Nørskov, J. K. *Nature Chem.* **2009**, *1*, 552.
13. Stamenkovic, V. R.; Mun, B. S.; Arenz, M.; Mayrhofer, K. J. J.; Lucas, C. A.; Wang, G.; Ross, P. N.; Marcoviæ, N. M. *Nature Mater.* **2007**, *6*, 241.
14. Fox, E. B.; Colon-Mercado, H. R. *Int. J. Hydrogen Energy* **2010**, *35*, 3280.
15. Kadirgan, F.; Kannan, A. M.; Atilan, T.; Beyhan, S.; Ozenler, S. S.; Suzer, S.; Yörür, A. *Int. J. Hydrogen Energy* **2009**, *34*, 9450.
16. Chen, W.; Kim, J.; Sun, S.; Chen, S. *J. Phys. Chem. C* **2008**, *112*, 3891.
17. Yoo, S. J.; Kim, S.-K.; Jeon, T.-Y.; Hwang, S. J.; Lee, J.-G.; Lee, S.-C.; Lee, K.-S.; Cho, Y.-H.; Sung, Y.-E.; Lim, T.-H. *Chem. Commun.* **2011**, *47*, 11414.
18. Hwang, S. J.; Yoo, S. J.; Jang, S.; Lim, T.-H.; Hong, S. A.; Kim, S.-K. *J. Phys. Chem. C* **2011**, *115*, 2483.
19. Hwang, S. J.; Yoo, S. J.; Jeon, T.-Y.; Lee, K.-S.; Lim, T.-H.; Sung, Y.-E.; Kim, S.-K. *Chem. Commun.* **2010**, *46*, 8401.
20. Kim, J. W.; Heo, J. H.; Hwang, S. J.; Yoo, S. J.; Jang, J. H.; Ha, J. S.; Jang, S.; Lim, T.-H.; Nam, S. W.; Kim, S.-K. *Int. J. Hydrogen Energy* **2011**, *36*, 12088.
21. Kim, J. W.; Lim, B.; Jang, H.-S.; Hwang, S. J.; Yoo, S. J.; Ha, J. S.; Cho, E. A.; Lim, T.-H.; Nam, S. W.; Kim, S.-K. *Int. J. Hydrogen Energy* **2011**, *36*, 706.
22. Jeon, T.-Y.; Yoo, S. J.; Cho, Y.-H.; Lee, K.-S.; Kang, S. H.; Sung, Y.-E. *J. Phys. Chem. C* **2009**, *113*, 19732.
23. Yang, J.; Deivaraj, T. C.; Too, H.-P.; Lee, J. Y. *Langmuir* **2004**, *20*, 4241.
24. Loukrakpam, R.; Luo, J.; He, T.; Chen, Y.; Xu, Z.; Njoki, P. N.; Wanjala, B. N.; Fang, B.; Mott, D.; Yin, J.; Klar, J.; Powell, B.; Zhong, C.-J. *J. Phys. Chem. C* **2011**, *115*, 1682.
25. Chen, M.; Feng, Y.-G.; Wang, X.; Li, T.-C.; Zhang, J.-Y.; Qian, D.-J. *Langmuir* **2007**, *23*, 5296.
26. Huang, Y.; Wang, W.; Liang, H.; Xu, H. *Cryst. Growth Des.* **2009**, *9*, 858.
27. Shao, M.; Sasaki, K.; Marinkovic, N. S.; Zhang, L.; Adzic, R. R. *Electrochem. Commun.* **2007**, *9*, 2848.
28. Gupta, G.; Slanac, D. A.; Kumar, P.; Wiggins-Camacho, J. D.; Wang, X.; Swinnea, S.; More, K. L.; Dai, S.; Stevenson, K. J.; Johnson, K. P. *Chem. Mater.* **2009**, *21*, 4515.